Available online at www.sciencedirect.com
SCIENCE DIRECT®
International Journal of Thermal Sciences 42 (2003) 455–469
International Journal of Thermal Sciences
www.elsevier.com/locate/ijts

Influence of the flow rate and the tank stratification degree on the performances of a solar flat-plate collector

C. Cristofari *, G. Notton, P. Poggi, A. Louche

Centre de recherches "énergie et systèmes", Université de Corse, U.M.R. CNRS 6134, route des Sanguinaires, 20000 Ajaccio, France

Received 28 August 2001; accepted 8 July 2002

Abstract

Using a thermal model of finite differences, the performances of a solar flat-plate thermal collector wholly manufactured in a copolymer material is studied in low flow conditions. The influences of the flow rate and the stratification of the tank are analysed. Thermal performances, productivity and efficiency of such a solar system (collector with surface of 2 m^2 and a storage tank of 150 litres) are presented for a Mediterranean site. Such a system presents a yearly mean efficiency of about 55.5% and 53.0% and the annual mean of daily productivities are 4.98 kWh and 4.75 kWh for, respectively, high thermal stratified tank and fully mixed tank.

These results show that a stratified tank has much higher performances than a fully mixed tank. With high degree of stratification saving energy is higher (5.25% over one year of use) than fully mixed tank. The use of polymer materials reduces the collector weight by 50% in comparison with a traditional metal collector, what implies an easier installation.

Keywords: Solar flat-plate collector; Copolymer; Stratified tank; Flow rate; Modeling; Performance

1. Introduction

Solar water heating systems have reached technical maturity and are used in many countries. After the first oil crisis in 1973, the strategies used by industrialised and developing countries to reduce their oil dependence have been numerous. A diversification of energy import, a structural change of the large domestic product (industrial development of activities using a low energy expenditure) or an increase of the national supply have been the essential measures taken by the countries with various degree of importance.

The island character of Corsica in Mediterranean sea (particularly the fact that this island is not connected to the French continental electrical grid) caused this region to opt for an energy sources diversification [1]. Natural resources of hydroelectric energyprovide about 30% of the island electrical's demand, two fuel thermal power plants meet 50% of demand and the remaining 15% are brought to Corsica from Italy via the SACO electrical cable.

This particularly character also induces a great gap between the production and distribution cost of electricity (identical in all over the French territory, 0.192 €·kWh^{-1}) against 0.12 €·kWh^{-1} duty-free. So, each kWh sold in Corsica increases the deficit of the French utility EDF (66 M€ deficit for a turnover of 105 M€). To reduce this deficit, EDF favours in Corsica and in French overseas territories (with the same EDF deficit) actions to reduce electricity consumption.

In this context, since the early 80s, the French Agency for Environment and Energy Management (ADEME) and the Corsican Territorial Collectivity have implemented a common policy consisting of financial aids for the development of renewable energies and actions to control and reduce energy cost.

This policy of aids (FCME) allows to develop the thermal solar energy in individual and collective applications. Today, respectively, 1200 m^2 and 3000 m^2 of solar collectors have been installed in individual and collective houses.

The low integration of thermal solar energy in Corsica

* Corresponding author.
E-mail addresses: cristofa@univ-corse.fr (C. Cristofari), notton@vignola.univ-corse.fr (G. Notton), poggi@vignola.univ-corse.fr (P. Poggi), louche@vignola.univ-corse.fr (A. Louche).

1290-0729/03/$ – see front matter
doi:10.1016/S1290-0729(02)00046-7

Nomenclature

A	surface area	m^2
b_0	numerical constant	
B	collector control function	
CC	thermal capacity	W·K^{-1}
C	specific heat capacity	J·kg^{-1}·K^{-1}
D	hydraulic diameter	m
DT	temperature difference, $= T_f - T_{ae}$	K
$DT1$	temperature difference, $= T_{2f} - T_{1f}$	K
e	thickness	m
E	energy gain by the fluid	kWh
G	total solar radiation ($\beta = 45°$)	W·m^{-2}
h	heat transfer coefficient	W·m^{-2}·K^{-1}
I	instantaneous incident solar radiation on the horizontal plane	W·m^{-2}
K	incidence angle modifier	
L	lenght	m
$\dot{m}$	collector mass flow rate	kg·s^{-1}·m^{-2}
M	material or fluid weight	kg
Pr	Prandtl number	
q	heat carried by the heater fluid	W
r	resistance	K·W^{-1}
R	geometric factor	
Re	Reynolds number	
S	solar energy absorption rate	W·m^{-2}
t	time	s
T	temperature	K
U	heat loss coefficient	W·m^{-2}·K^{-1}
V	wind speed	m·s^{-1}

Greek letters

α	absorptivity	
β	inclination of the collector	°
ε	emissivity	
Δ	inter node spacing	m
ϕ	potential sources or wells	W
η	instantaneous or Daily mean of efficiency	%
λ	thermal conductivity	W·m^{-2}·K^{-1}
θ	incidence angle	°
ρ	density	kg·m^{-3}
σ	Boltzmann constant	(5.6697·10^{-8} W·m^{-2}·K^{-4})
τ	transmittance	
υ	volume	m^3

Subscripts

a	inside air
ae	outside air
b	beam
c	collector
cd	conductive
cv	convective
d	diffuse
dp	dew point
eb	effective beam
ed	effective diffuse
eg	effective ground
f	fluid
g	ground
i	node (variables denoting certain parts of the system)
iso	insulation
j	node (variables denoting certain parts of the system)
l	inlet fluid in the tank from load
m	mean
n	normal
p	absorber
pb	bottom half of the absorber
pt	top half of the absorber
r	radiative
s	tank
sky	sky
w1	fluid in pipe *collector-tank*
w2	fluid in pipe *tank-collector*
0	total incident at the horizontal plane
1	inlet fluid in the collector from the tank
2	outlet fluid from collector
22	inlet fluid in the tank from collector

and more generally in France shows that a real environmental policy and more competitive prices of installations are necessary for a more extensive use of these systems.

In such way, we developed a copolymer solar collector whose thermal behaviour has been modeled and optimised using a finite difference model [2].

In this paper, we analyse more accurately the influence of the flow rate and consequently the stratification degree of the tank on the water heating system performances. The interest of this study resides in the approach used to model the tank and in the analyses of the number of the nodes used on the gained energy.

2. Literature review

2.1. Choice of the collector configuration

Various researches, developments and demonstration works on large-scale low cost plastic bag solar collectors have been realised since the seventies [3–5]. The system consisted in a plastic film water bag which rested on layer of thermal insulation. In 1997, Tsilingiris [6] proposed a solar collector based on the same principle but including a collector enclosure made with hard structural thermal insulation material.

Solar domestic hot water (SDHW) heaters are widely used today for collection of low temperature solar thermal energy. This type of collectors have been the subject of numerous studies and developments since 1950. Bliss [7] and Willier [8], Hottel and Willier [9] studied for the first time these solar collectors through the first thermal analyses for a parallel tubes collectors which served as a basis for many further developments.

An empirical equation to calculated the top heat loss coefficient from the collector plate was developed by Klein [10] following the basic procedure of Hottel and Woertz [11].

Hottel [9], Willier [8] and Bliss [7] elaborated relationships available for most collector designs (tube and sheet case) using an appropriate form of the collector efficiency factor.

Matrawy and Farkas [12] compared a two parallel plate collectors (TPPC), with respectively a parallel tubes collectors (PTC) and a serpentine tube collectors (STC). Under the same ambient and performance conditions, efficiency of the TPPC is respectively 6% and 10% greater than STC and PTC efficiency.

The authors explain performance of the TPPC by the uniform temperature distribution over the absorbed plate surface and the uniform distribution of the working fluid between the two plates. However, this comparison study has been performed for a plate thermal conductivity of different collectors equal to 211 $W{\cdot}m^{-1}{\cdot}K^{-1}$ corresponding to the use of expensive materials, for a configuration STC and a distance between tubes of 0.167 m.

The use of a polymer absorber has been studied by Van Nierkerk et al. [13] with the aim of evaluating the performances of parallel tubes collectors in south of Africa. The variation of geometrical variables such as tube diameter, tube spacing and pitch have been studied for optimising the collector performances. Van Nierkerk et al. [13] concluded that the best configuration is obtained for an inter tube spacing equal to zero. It appears that the configuration of the flat plate collector is the most important parameter which affects collector performance.

We propose in this paper to study the collector configuration which presents the highest performance similar to what proposed Hottel [9], Willier [8] and Bliss [7] and Matrawy and Farkas [12] but which differs mainly:

– in the choice of the low conductivity material used with the aim of having a solar collector which is corrosion resistant and not prone to scaling, of decreasing its weight and cost price;
– in its rectangular flow passageways conception in order to increase its toughness;
– in the calculation, heat capacities of the various components are taken into account and allows to make dynamical simulation of system behaviour.

2.2. Choice of the low flow SDHW design

Low flow SDHW systems differ from traditional SDHW system by having low volume flow rates in the solar collector loop of the systems. This configuration has several advantages comparing with a traditional operation (high flow) at various levels:

– *Thermal stratification:* Using low flow operation results in an increased outlet temperature from the solar collector and consequently induces a higher degree of thermal stratification inside the heat storage; Moreover, the temperature at the top of the storage will be closer to the desired load temperature. Therefore, the auxiliary energy consumption will be decreased which increases the solar fraction. Further, with highly stratified heat storage the return temperature to the solar collector will be lowered and the working periods for the solar collector will be longer, which implies in an increased output energy from the solar collector [14, 15].
– *Piping in the solar collector loop:* With low flow systems it is possible to use smaller pipes, in this way at first less material is used for pipes and insulation and secondly the heat losses are reduced.
– *Pump:* The energy consumption of the circulation pump is decreased.

The design of low flow SDHW systems varies from one country to another, which is due to differences in [16]:

- Regulatory issues concerning hot water systems;
- Design of conventional hot water systems;
- Available conventional energy sources and energy prices;
- Local conditions and traditions;
- Hot water consumption and patterns;
- The climate variations from one country to another.

The Canadian and North American low flow SDHW systems are normally based on pre-heating tank and an auxiliary tank.

In northern of Europe, low flow systems are often based on vertical mantle tank. The heat exchange between the solar collector fluid and the consumption water takes place in the mantle.

In central Europe, to obtain a very good stratification, a manifold diffuser is often used but this type of system is very expensive also compared to the increased performance initiated by the fine thermal stratification. However, in order to study the influence of thermal stratification in the tank, we will opt for this last configuration.

3. Description of the solar system

We consider a classical solar water heating installation with a flat-plate solar collector and a water tank for storage as shown in Fig. 1. A bypass is required which is controlled by a differential controller turning on the inlet fluid in the tank when the temperature T_{22f} is greater than the temperature of the fluid in the tank $T_{s,i}$ corresponding to the lowest temperature (at the bottom of the tank). If T_{22f} is lower than $T_{s,i}$, the fluid return to the collector [17].

The studied flat plate water collector is composed of a transparent cover and an absorber-exchanger which transform the solar radiation to heat. This "absorber-exchanger" has back and side insulations (in expanded polyurethane, $\rho_{iso} = 80$ kg·m^{-2}, $\lambda_{iso} = 0.022$ W·m^{-1}·K^{-1}), which is inserted in the body of the collector which allows a good mechanical behaviour of the collector structure as shown in Fig. 2.

The fluid is distributed uniformly under the surface of the absorber. The water flows are parallel. A header pipe supplies each pipe and another one collects the warm fluid. The pipes are connected to the system users as shown in Fig. 1.

The absorber-exchanger, made of copolymer material, must satisfy the following constraints: UV protected, high thermal conductivity, water-resistant and glycol-resistant (anti-freezing solution), good thermal range of utilisation ($-10\,°C \leftrightarrow 150\,°C$), a good mechanical strength and to be chemically stable.

Various anti-UV treated copolymers such as polycarbonate, polyphenylen ether or methyl polymethacrylate satisfy all these criteria. However, for our study, we selected the anti-UV treated polycarbonate which is the cheapest polymer and which satisfies chemical, mechanical and thermal constraints. All the properties of this copolymer are summarised in Table 1. We chose a single glass cover plate with a thickness equal to 4 mm.

4. Theoretical analysis: Equations and resolution

We present a model of finite differences which includes the essential thermal transfers. This model is composed of a serial assembling of many elementary models. Each model is based on a nodal discretisation of a collector section and of the storage circuit.

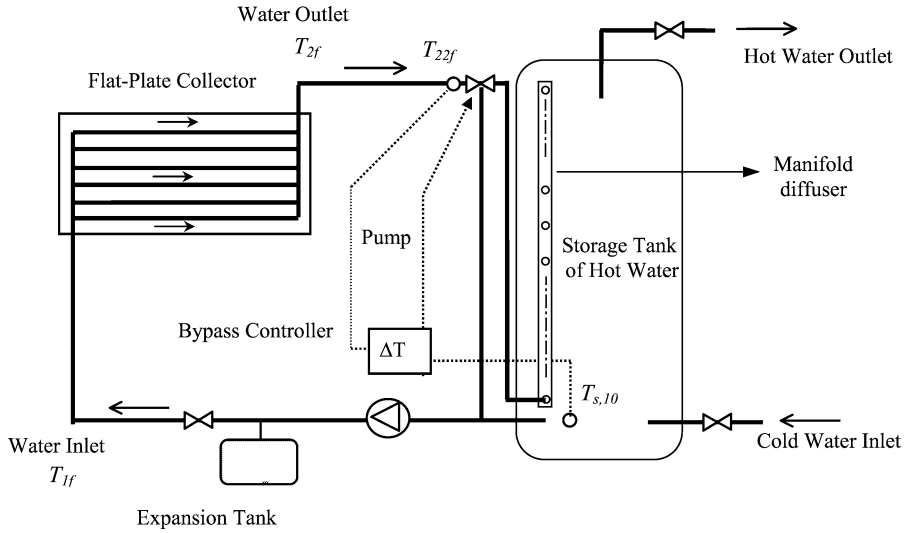

Fig. 1. Layout of the solar system installation.

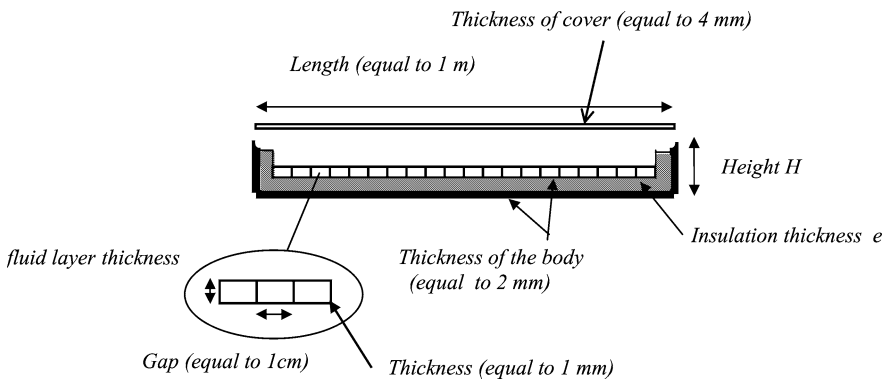

Fig. 2. Transversal section of the polymer collector. Schematic section of the pipes (in the flow direction).

Table 1
Properties of polycarbonate

Properties	Units	Polycarbonate copolymer
Physical		
Density	$kg{\cdot}m^{-3}$	1.18
Water absorption	%	0.15
Rate of cristallinity	%	0
Mechanical		
Breaking constraint	MPa	65
Breaking elongation	%	7
Traction module	MPa	2250
Thermal		
Vitreous transition (T_g)	°C	150
Casting shrinkage	%	0.7–0.9
Thermal conductivity	$W{\cdot}m^{-1}{\cdot}K^{-1}$	0.7–0.85
Advantages		Good mechanical properties, good dimensional stability, even in humid atmosphere, large range of using temperature (−80 °C, +135 °C)

4.1. Presentation of the collector: Model and assumptions

The simulation is done by dividing the transversal section collector into six isothermal regions: the glass cover (G), the air layer (A), the top half of the absorber (P1), the water layer (F), the bottom half of the absorber (P2) and the insulation (I); therefore, we propose to dividing the length collector into ten sections f_k in order to take into account the temperature distribution of the working fluid inside the collector.

This model also takes into account the following input physical parameters:

- diffuse and direct solar irradiances I_d and I_b;
- temperature of the ambient outside air T_{ae};
- temperature of the inside air T_a of the house;
- air velocity in front of the collector V;
- sky temperature T_{sky} calculated from the following equation [18]:

$$T_{sky} = T_{ae}\left[0.8 + \frac{T_{dp}\cdot 273}{250}\right]^{1/4} \tag{1}$$

T_{dp}: the dew point temperature.

A detailed description of these regions is shown in Fig. 3 and in Fig. 4. A heat balance is done for each region. These equations are elaborated from a model based on an electrical analogy where temperatures, flows, flow sources and imposed temperatures are respectively analogous to potentials, currents, current generators and voltage generators. The model is based on the following assumptions:

- the thermo-physical properties in solids and fluids are constant;
- the conductive transfers are neglected compared to the convective and radiative exchanges in the fluid layer;
- in the water layer of the collector, the conductive and radiative transfers are neglected with regard to the convective ones;
- the radiative transfers are neglected compared to the convective ones on the bottom face of the collector.

4.1.1. Global equations

For each node, according to the Kirchoff's law:

$$CC_i\frac{dT_i}{dt} = \sum_j U_{ij}(T_j - T_i) + \phi \tag{2}$$

Where ϕ is the solar irradiance incident on the glass or on the top half of the absorber depending on the considered node.

The capacities CC_i come from the term of power variation $M_i C_i \frac{dTi}{dt}$ from the balance equation for the mesh point i

$$CC_i = M_i C_i = \rho_i C_i \upsilon_i \tag{3}$$

The conductive term from the discretisation of the term $\lambda_i A_i \frac{dTi}{dt}$ is expressed according to the Fourier's law by:

$$U_{ij} = \lambda_i A_i \frac{1}{\Delta_{ij}} \tag{4}$$

Where Δ_{ij} is the inter node spacing.

Concerning U_{ij}, if the material of the mesh point i is different from the material of the mesh point j, the conductivity is expressed like two serial electrical resistances. If we assume a good contact between these two materials, we have:

$$U_{ij} = \frac{U_i \times U_j}{U_i + U_j} \tag{5}$$

The convective term is given by the Newton's law

$$hA_{ij}$$

The radiative exchange term is given by

$$\sigma\varepsilon_i\alpha_j A_i R_{ij}\left(T_j^4 - T_i^4\right) \tag{6}$$

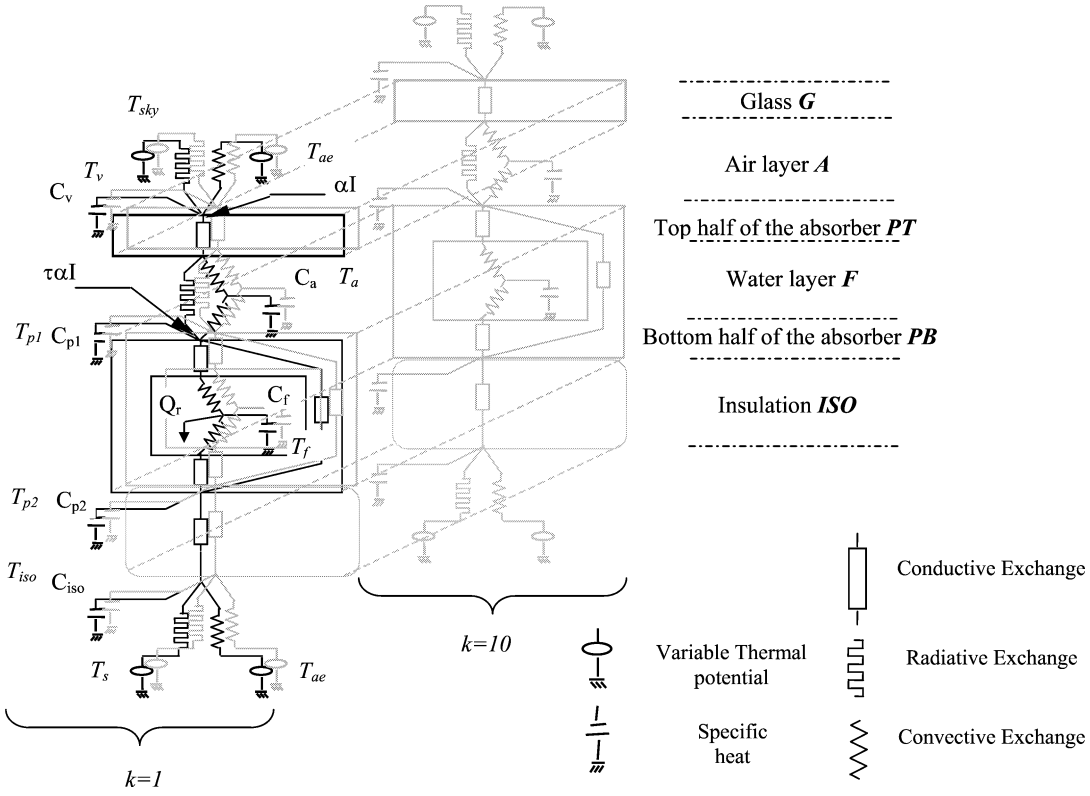

Fig. 3. Topologic diagram of the polymer collector.

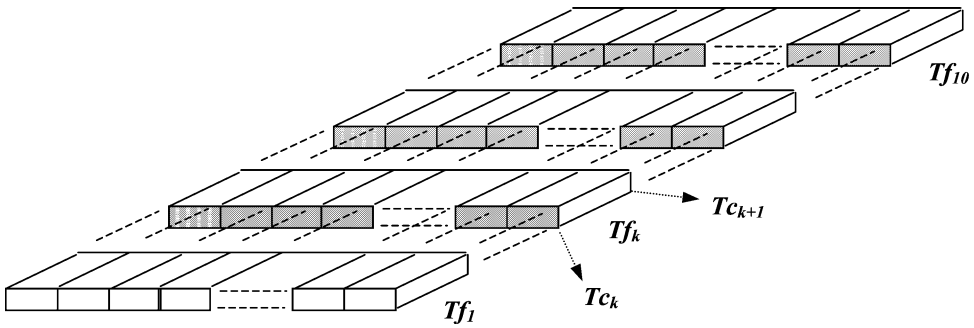

Fig. 4. Transversal section of the polymer absorber-exchanger.

where the different surfaces are considered as grey.

When the temperature difference $T_j - T_i$ is relatively small, the previous expression can be linearized to:

$$4\sigma\varepsilon_i\alpha_j A_i R_{ij}(T_j - T_i)T^3_{\mathrm{m},ij} \tag{7}$$

The radiative conductivity is then expressed by:

$$\begin{aligned} Ur_{ij} &= \sigma\varepsilon_i\alpha_j A_i R_{ij}\left(T_j^2 + T_i^2\right)(T_j + T_i) \\ &= 4\sigma\varepsilon_i\alpha_j A_i R_{ij} T^3_{\mathrm{m},ij} \end{aligned} \tag{8}$$

Lastly, the fluid transport is introduced into Eq. (2) by the factor $U_{\mathrm{f}}(T_i - T_j)$ where $U_{\mathrm{f}} = \dot{m}_{\mathrm{c}} C_f$.

More particularly, in the collector the fluid transport is introduced by $U_{\mathrm{f}}(Tc_{k+1} - Tc_k)$. The different expressions of temperature difference are given by

$$\begin{aligned} &Tc_{2k+1} - Tc_{2k} \\ &\quad = 2Tf_{2k+1} - 4\sum_{j=1}^{k} Tf_{2j} + 4\sum_{j=1}^{k} Tf_{2j-1} - 2T_{1\mathrm{f}} \end{aligned} \tag{9}$$

$$\begin{aligned} &Tc_{2k} - Tc_{2k-1} \\ &\quad = 2Tf_{2k} - 4\sum_{j=1}^{k} Tf_{2j-1} + 4\sum_{j=1}^{k} Tf_{2j-2} + 2T_{1\mathrm{f}} \end{aligned} \tag{10}$$

with Tf_k the average temperature in each section k of the collector ($k \in [1, 10]$):

$$Tf_k = \frac{(Tc_{k+1} + Tc_k)}{2} \tag{11}$$

The natural and forced convective coefficients and the configuration factors are estimated from classical correlations.

The following relation [19] describes the convective thermal exchanges inside the collector pipes, for the laminar flow regime:

$$h_f = \frac{\lambda_f}{D} 1.607 \left(\frac{D}{L_c} Re\, Pr \right)^{1/3} \quad \text{for } Re < 2300 \tag{12}$$

The convective transfer coefficient on the outside collector surface is related to the wind speed V by the relation [20]:

$$h_c = 7.0 + 2.1V \tag{13}$$

Among all the elements taken into account in the total coefficients of the thermal transfer, two terms allow to justify the choice of a collector with an absorber using polymer material. The first one depends on the conductivity of the layer crossed by the thermal flux, and the second one depends on the convective transfer coefficient between the surface which is in contact with the fluid and the fluid itself. But, the first is much greater than the second. Thus, we propose an 'absorber-exchanger' in copolymer material, poor heat conductor, but which can be used with a low thickness.

4.1.2. Meteorological data and solar energy absorption assumptions

The results presented are determined from real meteorological data collected in our laboratory situated at Ajaccio, a seaside Mediterranean site (Latitude 41°55′N, Longitude 8°48′). In this site, we have a complete meteorological station, where the direct normal and the global horizontal and tilted (30°, 45° and 60°) irradiances are respectively measured by an Eppley NIP pyrheliometer and a Kipp and Zonen (CM5) pyranometer. The standardisation of such instruments is maintained by the French meteorological organisation Meteo France. Other parameters such as ambient temperature, pressure, relative humidity, wind speed and direction are also recorded. The data are collected every minute and recorded. The diffuse radiation is not measured, but can be obtained easily from the following:

$$I_d = I - I_b \tag{14}$$

where I_d, I and I_b are respectively the diffuse, total and beam solar irradiance. We supposed that the collector faced to the south and 45° tilted [17].

The calculation of the absorbed solar irradiance S is based on the ASHRAE convention [21] and used by Tsilingiris [22]:

$$S = (\tau\alpha)_n \left(R_b I_b K_b + I_d K_d \frac{1+\cos\beta}{2} + (I_b + I_d)\rho_g K_g \frac{1-\cos\beta}{2} \right) \tag{15}$$

the incidence angle modifier for the direct component of solar radiation is given by:

$$K_b = 1 + b_0 \left(\frac{1}{\cos\theta_{eb}} - 1 \right) \tag{16}$$

θ_{eb} is the incidence angle of the beam solar radiation and the numerical constant $b_0 = -0.1$ is for single glazed collectors.

For the sky and ground diffuse radiation, this coefficient is given as a function of the diffuse radiation equivalent sky and ground incidence angles:

$$K_d = 1 + b_0 \left(\frac{1}{\cos\theta_{ed}} - 1 \right) \tag{17}$$

$$K_g = 1 + b_0 \left(\frac{1}{\cos\theta_{eg}} - 1 \right) \tag{18}$$

The equivalent sky and ground incidence angles for diffuse radiation are given as a function of the collector field tilt angle and calculated according to Duffie and Beckman [23]:

$$\theta_{ed} = 59.68 - 0.1388\beta + 0.001497\beta^2 \tag{19}$$

$$\theta_{eg} = 90 - 0.5788\beta + 0.002693\beta^2 \tag{20}$$

with the inclination of the collector $\beta = 45°$ and the ground albedo $\rho_g = 0.2$ for our site. The normal transmittance-absorbance is fixed at 0.80.

4.2. Presentation of the tank: Model and assumptions

Water tank may operate with significant degrees of stratification with the top of the tank hotter than the bottom. In our case, the tank will be modeled in i sections (i nodes), [23] with energy balances written for each section of the tank.

To formulate these equations, we make assumptions about how the water entering the tank is distributed to the various nodes.

The water from the collector and from the load enter respectly at a temperature T_{22f} and T_l. It can be assumed that all water finds its way down inside the tank from node 1 to node i, where its density is nearly equal to the density of the water in the tank corresponding to the node i. To obtain this configuration, we use a manifold diffuser (Fig. 1) [16].

A collector control function B_c^i can be defined to determine which node receives collector return water:

$$B_c^i = \begin{cases} 1 & \text{if } i = 1 \text{ and } T_{22,f} > T_{s,i} \\ 1 & \text{if } T_{s,i-1} \geqslant T_{22,f} > T_{s,i} \\ 0 & \text{if } i = 0 \text{ or } i = N + i \\ 0 & \text{otherwise} \end{cases} \tag{21}$$

The i branches of the collector return water are controlled by this collector return control function as shown in Fig. 5.

The liquid returning from the load can be controlled in a similar manner with a load return control function B_l^i.

$$B_l^i = \begin{cases} 1 & \text{if } i = N \text{ and } T_l < T_{s,N} \\ 1 & \text{if } T_{s,i-1} \geqslant T_l > T_{s,i} \\ 0 & \text{if } i = 0 \text{ or } i = N + 1 \\ 0 & \text{otherwise} \end{cases} \tag{22}$$

The net flow between nodes can be either up or down depending upon the magnitudes of the collector and load

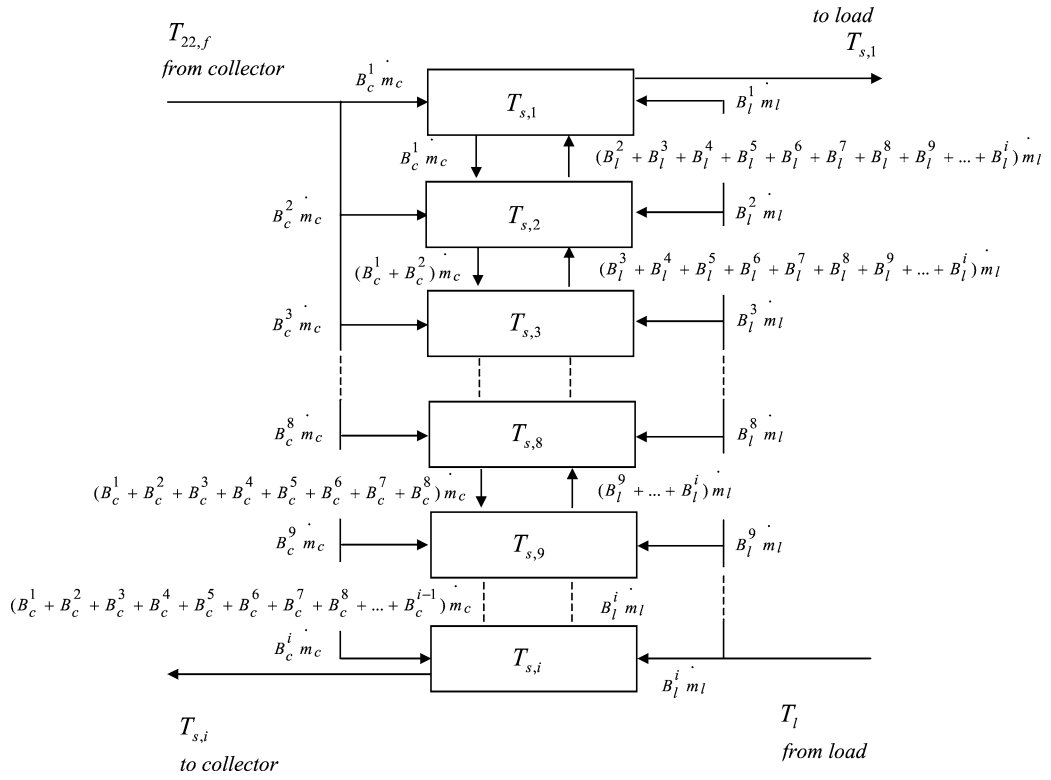

Fig. 5. i nodes stratified liquid storage tank.

flow rates and the values of the two control functions at any particular instant. It is convenient to define a mixed flow rate that represents the net flow into node i from node $i-1$, excluding the effects of flow, if any, directly into the node from load

$$\begin{cases} \dot{m}_{\mathrm{m},1} = 0 \\ \dot{m}_{\mathrm{m},i} = \dot{m}_{\mathrm{c}} \sum_{j=1}^{i-1} B_{\mathrm{c}}^{j} - \dot{m}_{l} \sum_{j=i+1}^{N} B_{l}^{j} \\ \dot{m}_{\mathrm{m},N+1} = 0 \end{cases} \tag{23}$$

With control functions defined above, an energy balance on node i can be expressed as:

$$\begin{aligned} &\rho_i C_i v_i \frac{\mathrm{d}T_{\mathrm{s},i}}{\mathrm{d}t} \\ &\quad = U_{\mathrm{s}}(T_{\mathrm{a}} - T_{\mathrm{s},i}) + B_{\mathrm{c}}^{i} \dot{m}_{\mathrm{c}} C_i (T_{22,\mathrm{f}} - T_{\mathrm{s},i}) \\ &\qquad + B_{l}^{i} \dot{m}_{l} C_i (T_l - T_{\mathrm{s},i}) \\ &\qquad + \begin{cases} \dot{m}_{\mathrm{m},i} C_i (T_{\mathrm{s},i-1} - T_{\mathrm{s},i}) & \text{if } \dot{m}_{\mathrm{m},i} > 0 \\ \dot{m}_{\mathrm{m},i+1} C_i (T_{\mathrm{s},i} - T_{\mathrm{s},i+1}) & \text{if } \dot{m}_{\mathrm{m},i+1} < 0 \end{cases} \end{aligned} \tag{24}$$

where a term $U_{\mathrm{s}}(T_{\mathrm{a}} - T_{\mathrm{s},i})$ has been added to take into account the heat losses from node i to the environment (house) at the temperature T_{a} assumed constant and equal to 20 °C.

This model is based on the following assumption: the conductive transfers of the manifold diffuser is neglected compared to thermal exchange of mixed flow.

The various simulations have been developed for a normalised water consumption profile corresponding to an evening demand for which the hot water is totally used from 18 hours.

4.3. Connection pipes

Modeling the connection pipes with insulation ($e = 3$ cm) is simplified by considering the energy balance as a whole for the liquid returning from the load and returning from the collector. The temperature developments in the pipe connections are assumed linear. Thus, the energy balance can be described as:

$$\begin{aligned} LC_{\mathrm{f}} \frac{\mathrm{d}T_{\mathrm{w1}}}{\mathrm{d}t} &= \dot{m}_{\mathrm{c}} C_{\mathrm{f}} (T_{22\mathrm{f}} - T_{2\mathrm{f}}) + U_{\mathrm{p}} L_{\mathrm{wae}} (T_{\mathrm{ae}} - T_{\mathrm{w1}}) \\ &\quad + U_{\mathrm{p}} L_{\mathrm{wa}} (T_{\mathrm{a}} - T_{\mathrm{w1}}) \end{aligned} \tag{25}$$

$$\begin{aligned} LC_{\mathrm{f}} \frac{\mathrm{d}T_{\mathrm{w2}}}{\mathrm{d}t} &= \dot{m}_{\mathrm{c}} C_{\mathrm{f}} (T_{1\mathrm{f}} - T_{\mathrm{s},i}) + U_{\mathrm{p}} L_{\mathrm{wae}} (T_{\mathrm{ae}} - T_{\mathrm{w2}}) \\ &\quad + U_{\mathrm{p}} L_{\mathrm{wa}} (T_{\mathrm{a}} - T_{\mathrm{w2}}) \end{aligned} \tag{26}$$

$$L = L_{\mathrm{wae}} + L_{\mathrm{wa}} \tag{27}$$

We supposed a pipe length $L_{\mathrm{wae}} = L_{\mathrm{wa}} = 1.5$ m corresponding respectively to the part of pipe outside and inside the house.

4.4. Method of solution

All the energy balances can be written in the guise of a differential matrix equation:

$$[C] \frac{\mathrm{d}\vec{T}(t)}{\mathrm{d}t} = [M]\vec{T}(t) + [S]\vec{E}(t) \tag{28}$$

$\vec{T}(t)$ is a vector containing system temperatures at the $62+i$ nodes ($T_{v_k}, T_{a_k}, T_{pt_k}, T_{f_k}, T_{pb_k}, T_{iso_k}, T_{w1}, T_{w2}, T_{si}$) of the mesh, $[C]$ is a diagonal matrix (dimension: $62+i$) with all the values of the thermal capacities of the material, $[M]$ is a squared matrix (dimension: $62+i$, with $i = 1, 3, 6, 10, 15$) with all the heat exchange coefficients between the elements of the mesh, $[S]$ is a matrix (dimension: $(62+i)\times 5$) which joins together the 5 input physical parameters (or excitations) expressed by the vector $\vec{E}(t)(I_b, I_d, T_{ae}, T_a, T_{sky})$ and $62+i$ elements of the mesh. By solving the equations of this analogical model, we get directly the expression of the temperature for each nodes of the model in function to the input parameters. This equation system is solved by the Runge Kutta Merson's method (order 4).

5. Results and discussion

The sizing must respond to the needs of hot water for 3 inhabitants in a Mediterranean site. Thus, we considered a collector with a surface of 2 m^2, a storage tank of 150 litres. All the temperatures of the incoming water in the tank are summarised in Table 2. The simulations have been performed with one year of real weather data. It is assumed that, in the early morning, the water inside the collector and all the parts of the collector follow the ambient temperature and the temperature of the water inside the tank are given in Table 2.

To take into account in the modeling the degree of tank stratification, it is necessary to divide the tank in a given number of nodes. Obviously, if the tank is fully mixed, the temperature at these various i nodes will be the same one whatever the number orifices of the manifold diffuser is. More the degree of stratification is high, more the number i of nodes (and so orifices) will have to be high. Thus, we want to determine the optimal number of nodes needed to maximise correctly the performances of the low flow SDHW. In a second time, we will calculate the optimum flow rate allowing a maximum production of thermal energy.

5.1. Influence of the number of nodes used to model the tank

Fig. 6 show the influence of the number of nodes on the gained energy calculated on one year of data.

We modeled the tank using respectively 1, 3, 6, 10 and 15 nodes corresponding to the orifices number of the manifold diffuser. According to the number of nodes, the calculated performances are different. More the flow rate is low, more the degree of stratification in the tank is important. So, in order to take into account this stratification, the tank must be modeled with a sufficient number of nodes and consequently the manifold diffuser must have sufficient number of orifices. In fact, using only one node correspond to a homogenous temperature in the tank which is a wrong hypothesis for the low flow but becomes more realistic for high flow as seen in Fig. 6 where the gained energy is identical whatever the number of nodes is.

As a matter of fact, even with only one orifice, using low flow rate results in a thermal stratification.

We note that the modeling with 10 and 15 nodes conduces to the same results: so it seems to be not necessary to use more than 10 nodes and so, no more than 10 orifices, to study the behaviour of this solar domestic hot water. In the following of this article all the presented results will be computed with a ten nodes model for the tank and so with a manifold diffuser with ten orifices.

5.2. Influence of the flow rate

Using low flow operation results in an increased outlet temperature from the solar collector and a higher degree of thermal stratification inside the heat storage. We note that a stratified tank has much higher performance than a fully mixed tank.

The Fig. 6 show that the mixing caused by a high flow rate begin for about 30 $kg{\cdot}m^{-2}{\cdot}s^{-1}$ because from this flow rate value the results obtained with 1 and 10 nodes are similar.

For a stratificated tank, it appears an optimal flow rate equal to $2.65{\cdot}10^{-3}$ $kg{\cdot}m^{-2}{\cdot}s^{-1}$ (i.e., 0.12 tank volume per hour) which maximize energy saving.

With this flow rate conducing to a stratificated tank, the gained energy is 5.25% higher than a fully mixed tank. These results are close to results obtained by Furbo [14] in testing low flow solar heating.

Thus, the value of flow rate equal to 2.65×10^{-3} $kg{\cdot}m^{-2}{\cdot}s^{-1}$ seems to be adequate for our solar collector. This optimal value of the flow rate is used to determine the collected solar thermal energy and the daily mean of the efficiency over one year of use.

5.3. Daily dynamical evolution of fluid temperatures and efficiency

For a given geometrical configuration, for a given running mode (insulating thickness $e = 2$ cm, flow rate $\dot{m}_c = 2.65{\cdot}10^{-3}$ $kg{\cdot}m^{-2}{\cdot}s^{-1}$, fluid layer thickness equal to 1cm, [2]) and for a stratified tank (10 nodes), we show in Figs. 7 and 8 the daily evolution of the efficiency, the temperature of the output collector fluid and the temperature of the storage tank fluid for a summer day (August 25) and for a winter day (February 28).

The daily mean efficiency is given by the following relation [23]:

$$\eta_{day} = \frac{\sum q_f}{A_c \int_{sunrise}^{sunset} I(t)\,dt} \tag{29}$$

The simulation based on the August 25, shows that the important radiation (daily peak greater than 700 $W{\cdot}m^{-}2$) allows a constant energy supply during all the day to the storage tank from the collector. The Fig. 8 presents a variable

Table 2
Average temperature of the incoming water in the tank

Ajaccio 41°55′					
January	February	March	April	May	June
10 °C	10 °C	11 °C	14 °C	16 °C	18 °C
July	August	September	October	November	December
19 °C	20 °C	18 °C	16 °C	14 °C	11 °C

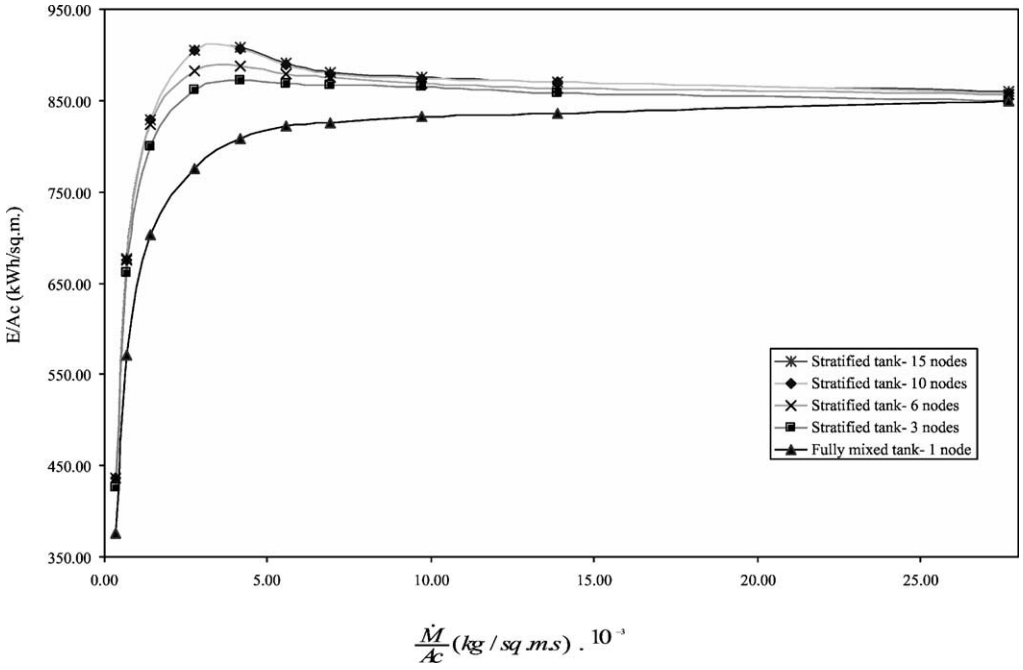

Fig. 6. Gained energy versus the flow rate of the fluid (with a thickness of insulation = 2 cm).

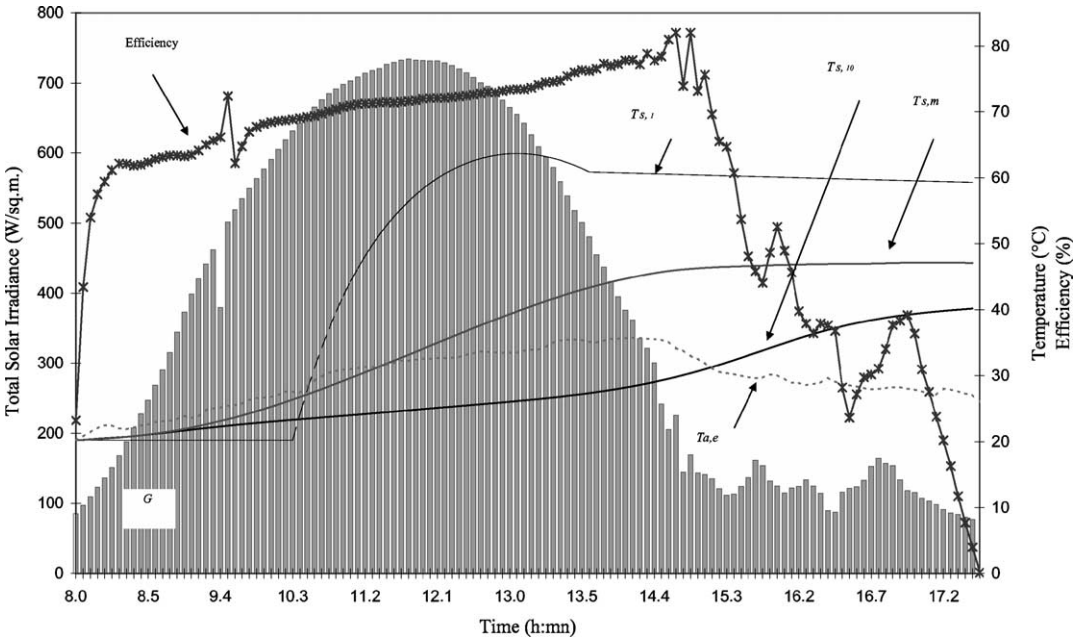

Fig. 7. Evolution of the efficiency and storage fluid temperature (August 25).

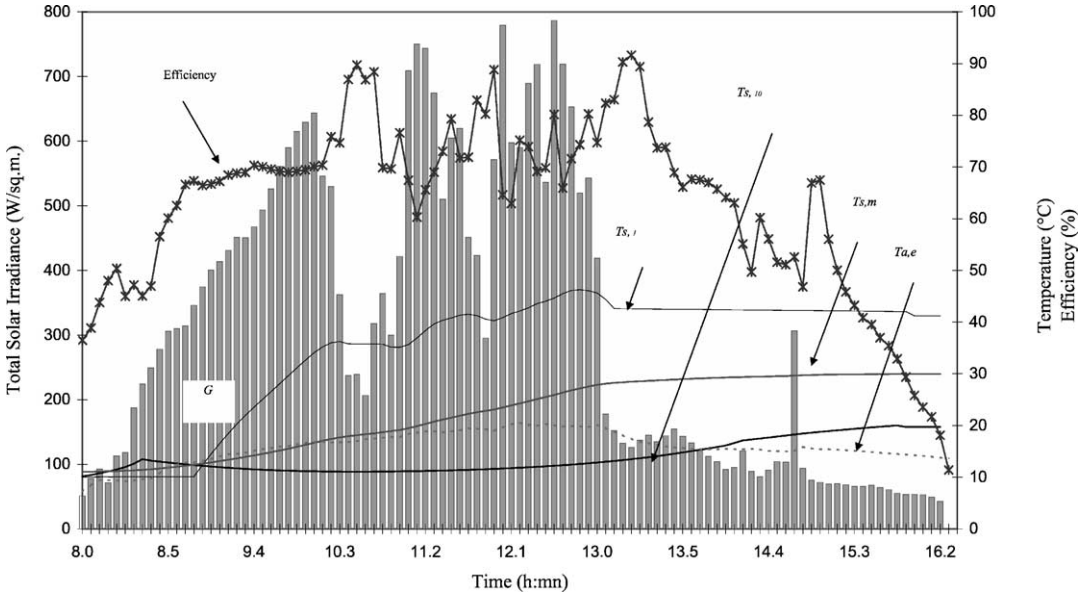

Fig. 8. Evolution of the efficiency and storage fluid temperature (February 28).

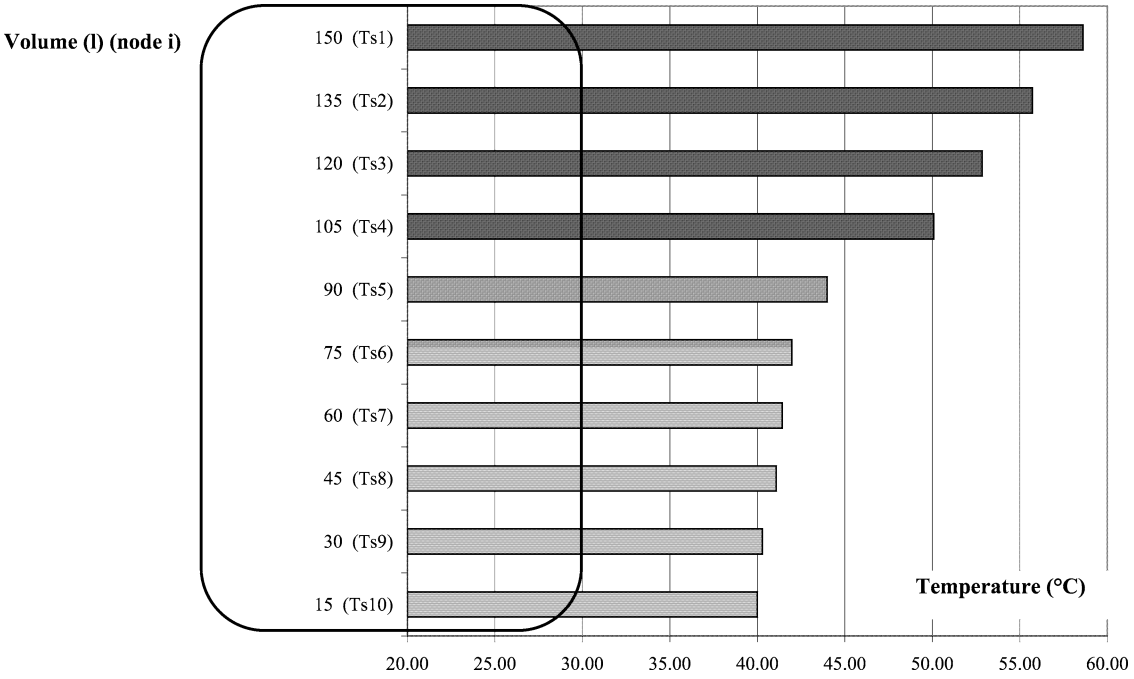

Fig. 9. Temperature profile in tank (August 25).

radiation due to cloud passages. We note a gain of energy in the storage fluid during the first half of the day. The water stays in the collector when the regulation is on, then the fluid temperature comes closer to the outdoor air temperature.

We note in Figs. 9 and 10 the temperature profiles in the tank for a summer day and a winter day; the final average temperatures in the storage tank are respectively about 48.0 °C (degree of stratification max $(T_{s,1} - T_{s,10}) = 19.5\,^{\circ}\mathrm{C}$) and 29.7 °C (degree of stratification max $(T_{s,1} - T_{s,10}) = 21.0\,^{\circ}\mathrm{C}$), and with 71% and 61.5% respectively of mean collector efficiencies, with a wind speed taken equal to $0\ \mathrm{m\cdot s^{-1}}$.

We see in Fig. 11 the temperature profile in the collector computed from simulations.

Fig. 12 illustrates for a summer day (august 25) the temperature difference between outlet and inlet fluid of the collector. It varies in the range from 0 °C to 7 °C for fully mixed tank and in the range from 0 °C to 40 °C for high thermal stratified tank. Using low flow operation, we

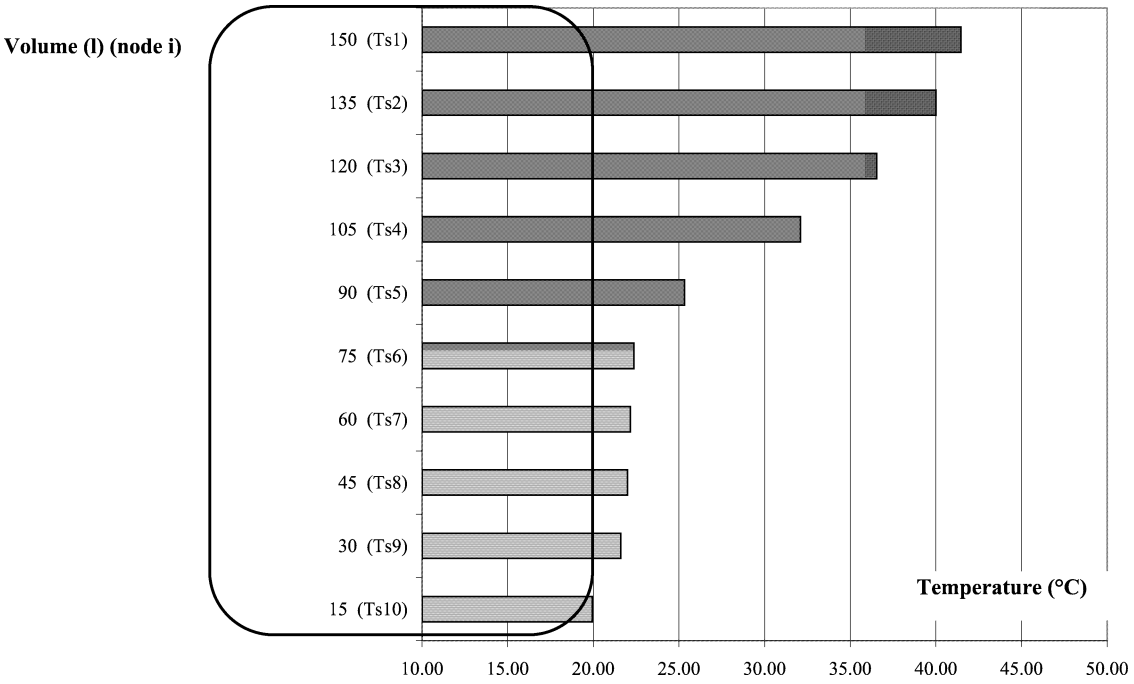

Fig. 10. Temperature profile in tank (February 28).

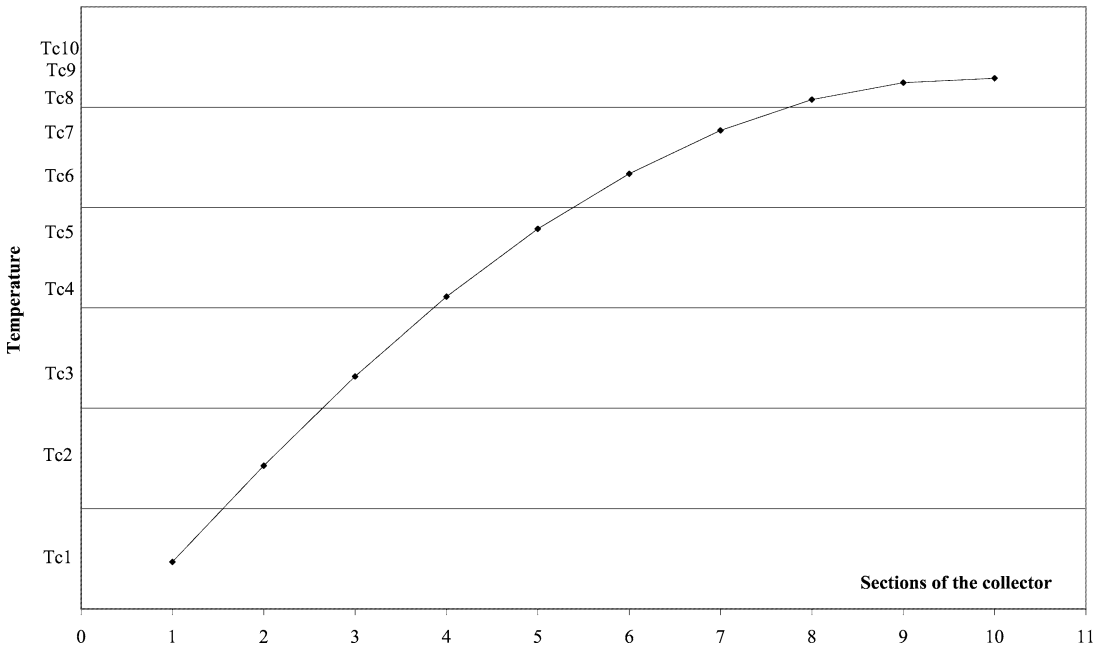

Fig. 11. Temperature profile in the collector.

note a working period for the solar collector longer than a conventional flow operation where temperature difference is about 0 °C during the last 2 hours and 30 minutes of the day.

Using low flow operation results in a decreased outlet temperature from the tank, a decreased of the annual mean of temperature solar collector (even if we note an increased outlet temperature from the solar collector) and so a decreased of DT and consequently a higher instantaneous efficiency of the system (Fig. 13).

Consequently, this low flow rate induces a thermal stratification of the tank which increase and maximise energy saving (Fig. 6).

5.4. Performance of the system

The flow rate has an important influence on the performances of the solar system. We studied this influence in calculating the average efficiency of the collector during five minutes (for a high thermal stratified tank $\dot{m}_c =$

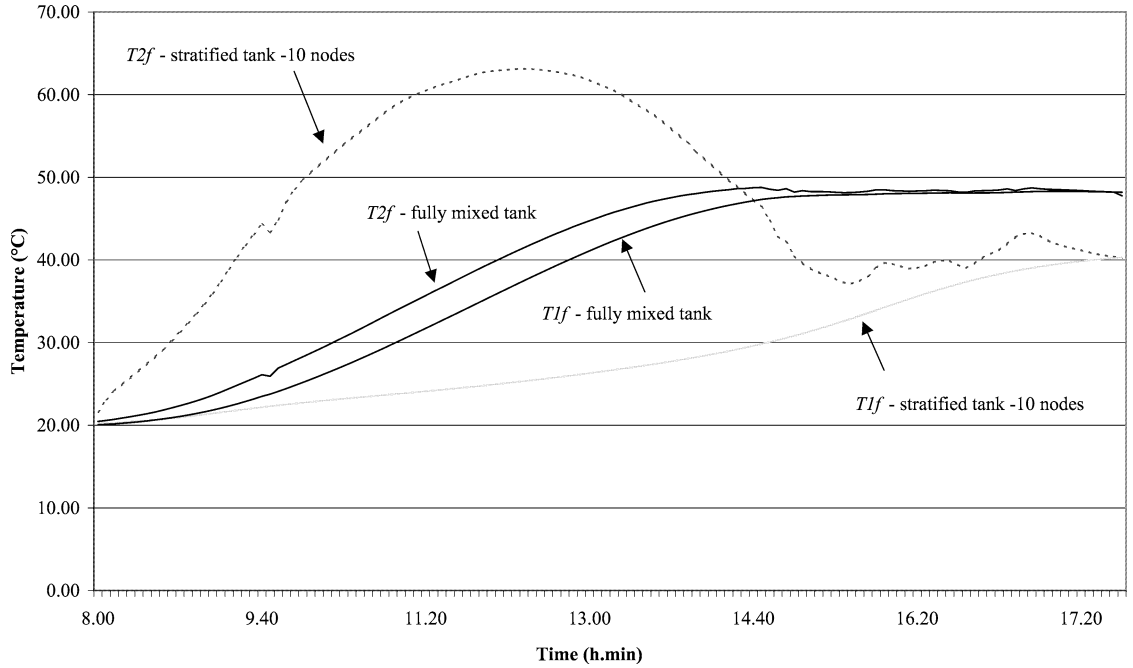

Fig. 12. Temperature evolution of outlet and inlet fluid of the collector for stratified tank and fully mixed tank.

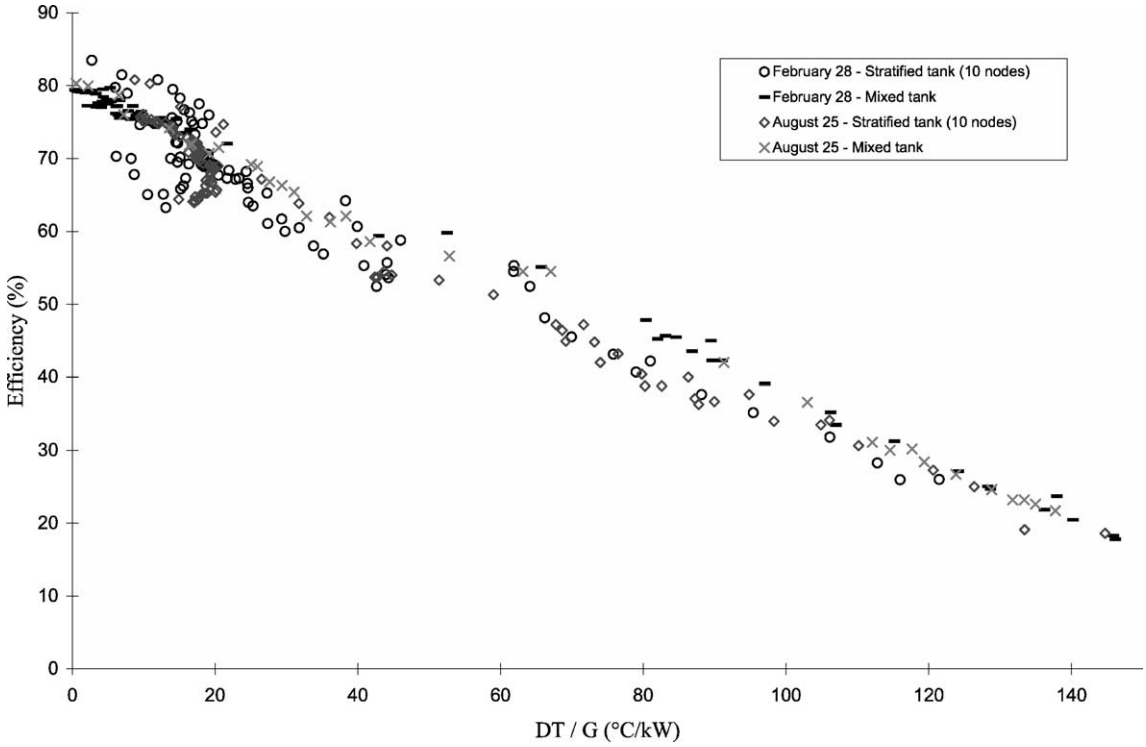

Fig. 13. Instantaneous efficiency versus the ration "DT/G" for fully mixed tank and stratified tank.

2.65×10^{-3} kg·m^{-2}·s^{-1} and for a fully mixed tank $\dot{m}_c = 30 \times 10^{-3}$ kg·m^{-2}·s^{-1}).

For two particular days (winter and summer), the Fig. 13 illustrates the effect of the flow rate on the response of the collector efficiency. This study has been performed on 365 days, we note a linear response of the efficiency [23] according to the flow operation:

when we used low flow operation, and so with high stratified tank, the working periods for the solar collector will be longer, which results in an increased nots in higher efficiency.

Equations of the straight lines (calculated by linear regression method on the basis of about 45000 points, i.e., 365 days) are respectively for fully mixed tank and

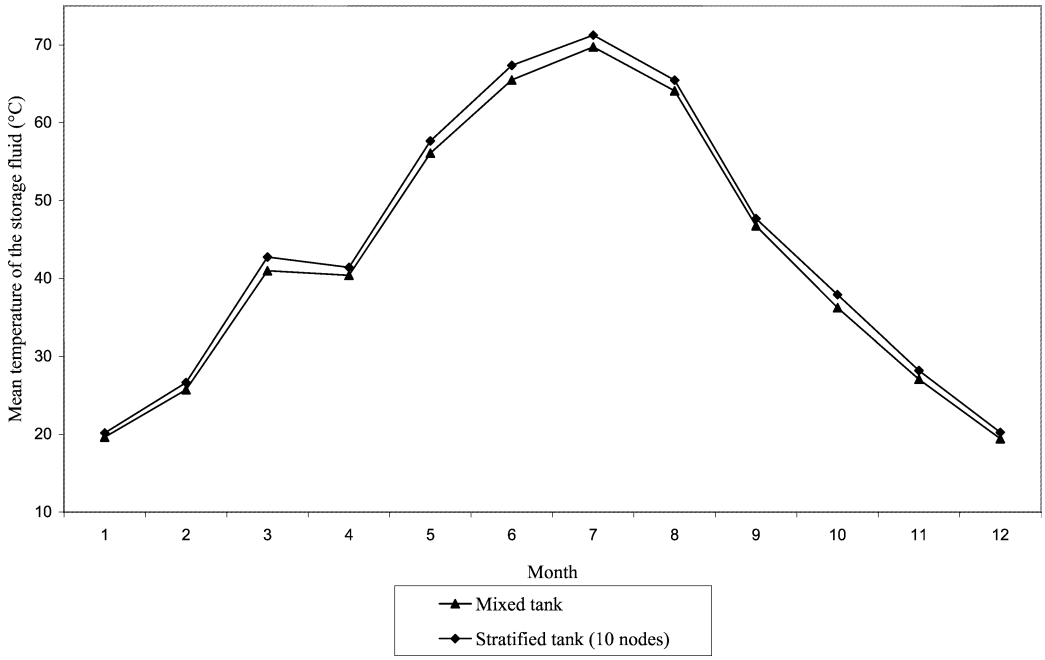

Fig. 14. Monthly mean temperature of the storage fluid for fully mixed tank and stratified tank.

Table 3
Daily mean energy and efficiency for fully mixed tank and stratified tank for each season

Seasons	Mean temperature	Daily mean solar energy (kWh) ($\beta = 45°$)	Stratified tank (10 nodes)		Mixed tank	
			Daily mean energy collected (kWh)	Daily mean efficiency (%)	Daily mean energy collected (kWh)	Daily mean efficiency (%)
Winter	9.6	6	3.06	50	2.88	48
Spring	16.2	11.79	6.48	55	6.25	53
Summer	23.6	12.51	7.63	61	7.38	59
Autumn	13.8	4.78	2.72	56	2.48	52

high stratified tank: $\eta = -0.41DT/G + 79.73$ and $\eta = -0.44DT/G + 77.82$.

Daily evolution of the available solar energy

For a solar collector with a surface of 2 m^2, from Table 3, the annual mean of daily efficiencies are 55.5% and 53.0% and the annual mean of daily productivities are 4.98 kWh and 4.75 kWh, respectively, for fully mixed tank and high stratified tank.

Fig. 14 illustrates during a year the evolution of monthly mean temperature of the storage fluid for fully mixed tank and high thermal stratified tank. These monthly mean temperatures vary in a range from 19.3 °C to 69.7 °C for fully mixed tank and in a range from 20.1 °C to 71.2 °C for high thermal stratified tank.

6. Conclusion

In this paper, we illustrated the thermal behaviour of a solar collector using a copolymer material in regard to radiative conditions. We chose a copolymer material for the 'absorber-exchanger' satisfying chemical, thermal and mechanical constraints: the polycarbonat.

We developed a nodal model for the solar water heating installation and studied the influence the flow rate and thermal stratification tank. The optimised system has an insulation of 2 cm, a thickness of 1 cm for fluid layer and works with a collector flow rate of 2.65×10^{-3} kg·m^{-2}·s^{-1}. Such a system presents a yearly mean efficiency of about 55.5% and 53.0% and the annual mean of daily productivities are 4.98 kWh and 4.75 kWh respectively for fully mixed tank and high thermal stratified tank.

The results show that ten orifices for the manifold diffuser are enough to have a high stratified tank and a stratified tank has much higher performance than a fully mixed tank. With high degree of stratification saving energy is higher (5.25% over one year of use) than fully mixed tank.

The utilisation of a copolymer for the total design of the solar collector has the advantage of reducing the weight by more half in comparison with a traditional collector using essentially metals with similar performances.

References

[1] C. Cristofari, P. Notton, G. Poggi, A. Louche, Diagnostic de la situation énergétique de la région Corse—L'éolien peut-il être intégré dans une réelle politique énergétique de développement?, Rev. Energie Ed. Tech. Econom. 521 (2000) 544–552.

[2] C. Cristofari, P. Notton, G. Poggi, A. Louche, Modeling and performance of a copolymer solar water heating collector, Solar Energy (2001), in press.

[3] W.C. Dickinson, A.F. Clark, J.A. Day, L.F. Wouters, The shallow solar pond energy conversion system, Solar Energy 18 (1976) 3–10.

[4] A.F. Clark, A.B. Casamajor, L.D. Hewett, Shalow solar ponds, in: Solar Energy Technology Handbook, Part A, New York, 1978, pp. 377–402.

[5] A.B. Casamajor, The application of shallow solar ponds for industrial process heat: Case histories, in: Proc. A.S./ISES Silver Jubilee Congress, Atlanta GA, 1979, pp. 1029–1032.

[6] P.T. Tsilingiris, Design, analysis and performance of low-cost plastic film large solar water heating systems, Solar Energy 60 (5) (1997) 245–256.

[7] R.W. Bliss, The derivations of sereval plate efficiency factors useful in the design of flat plate solar heat collectors, Solar Energy 3 (1959) 55–63.

[8] A. Willier, Prediction of performance of solar collectors, in: Applications of Solar Energy for Heating and Cooling of Buildings, ASHRAE, New York, 1977.

[9] H.C. Hottel, A. Whillier, Evaluation of flat plate collector performance, Trans. the Conference on the Use of Solar Energy University of Arizona Press 2 (1958) 1–74.

[10] S.A. Klein, Calculation of flat-plate collector loss coefficients, Solar Energy 17 (1975) 79–80.

[11] H.C. Hottel, B.B. Woertz, Performance of flat-plate solar-heat collectors, Trans. Amer. Soc. Mech. Engin. 64 (1942) 91–103.

[12] K.K. Matrawy, I. Farkas, Comparison study for three types of solar collectors for water heating, Energy Convers. Manag. 38 (1997) 861–869.

[13] W.M.K. Van Niekerk, C.G. du Toit, T.B. Scheffler, Performance modeling of a parallel tube polymer absorber, Solar Energy 58 (1996) 39–44.

[14] L.J. Shah, Investigation and modeling of thermal conditions in low flow SDHW systems, Department of Buildings and Energy Technical University of Denmark Report R-034, 1999.

[15] S. Furbo, Optimum design of small DHW low flow solar heating systems, ISES Solar World Congress Budapest Report 93-24, 1993.

[16] S. Furbo, Present and future SDHW System technology, in: Proceedings EuroSun '98, Portorôz, Slovenia, 1998.

[17] M. Chateauminois, D. Mandineau, D. Roux, Tableau des températures du réseau eau froide Calcul d'installations solaire à eau, Collection de l'ESIM Edition EDISUD, 1979.

[18] R.W. Bliss, Atmospheric radiation near the surface of the ground, Solar Energy 5 (3) (1961) 103–120.

[19] M.A. Lévêque, Les lois de transmission de chaleur par convection, Annal. Mines Mem. 13 (1928) 201–205.

[20] T. Schott, Operation temperatures of PV modules, in: Paper Presented to 6th PVSEC Conference, London, 1985, pp. 392–396.

[21] ASHRAE, Methods of Testing to Determine the Thermal Performance of Solar Collectors, ASHRAE, New York, 1997.

[22] P.T. Tsilingiris, Solar water heating design—A new simplified approach, Solar Energy 57 (1) (1996) 19–28.

[23] J.A. Duffie, W.A. Beckman, Solar Energy Thermal Processes, 2nd Edition, Wiley–Interscience, New York, 1991, ISBN 0-471-51056-4.